Supplementary Information

for

Synthesis and characterization of sodium hafnium oxide (Na_2HfO_3) and its high temperature CO_2 sorption properties

Ribooga Chang[a], Erik Svensson Grape[b], Teva Clairefond[a], Evgenii Tikhomirov[a], A. Ken Inge[b] and Ocean Cheung[a]*

[a] Division of Nanotechnology and Functional Materials, Department of Materials Science and Engineering, Uppsala University, Ångström Laboratory, Uppsala SE-751 03, Box 35, Sweden

[b] Department of Materials and Environmental Chemistry, Stockholm University, SE-10691, Sweden

*Corresponding author. Tel.: +46 18 471 3279, Email:ocean.cheung@angstrom.uu.se

Table of contents

Section 1. Synthesis of Sodium hafnium oxide (Na_2HfO_3)

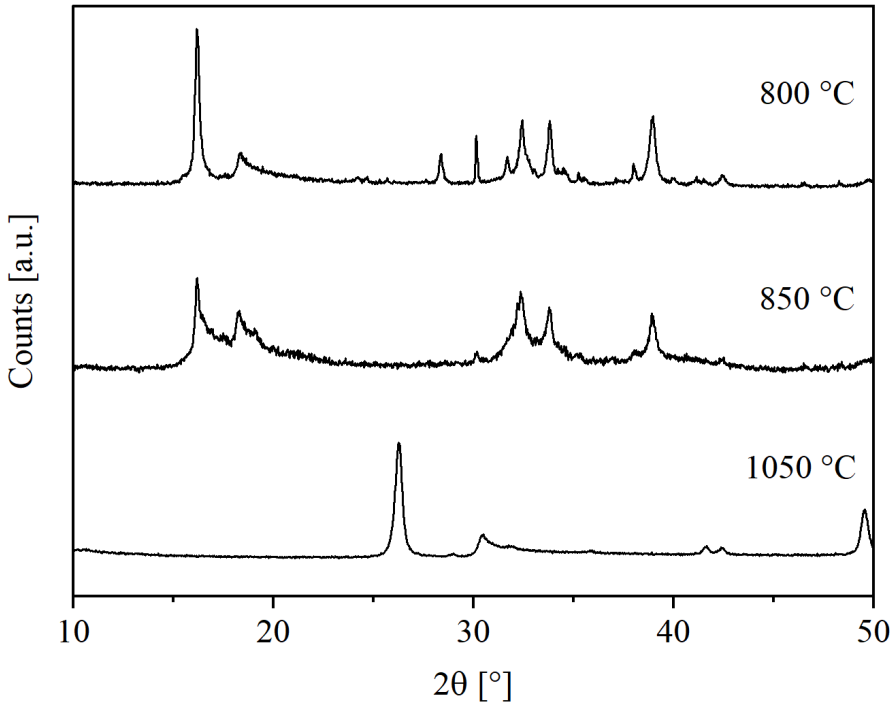

Figure S1. The synthesized NHO-1.25 by the different synthesis temperatures at 800, 850, and 1050 °C.

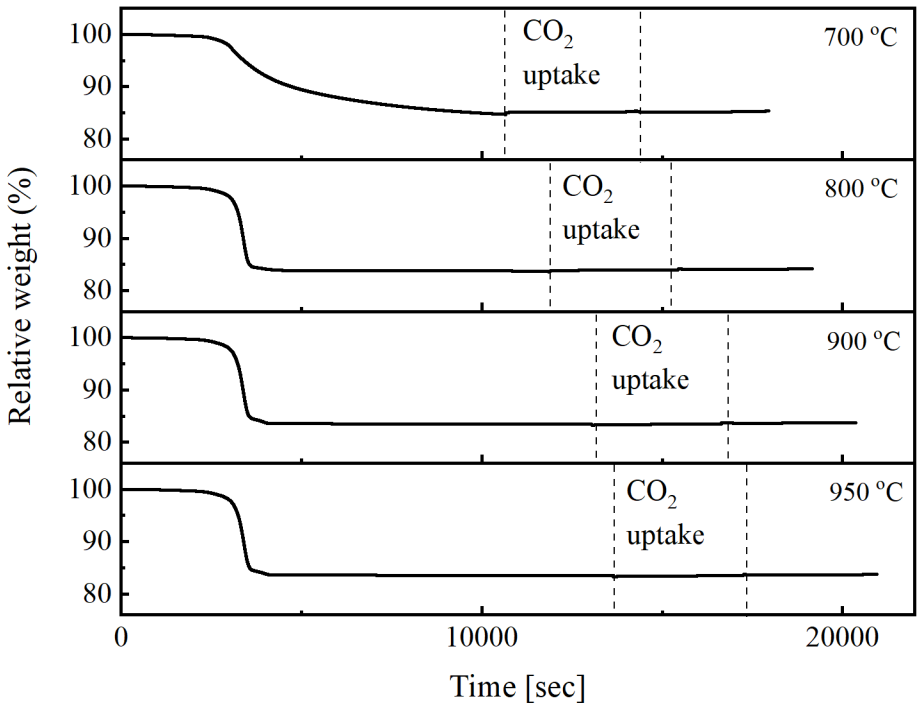

Figure S2. The synthesized Li_2HfO_3 under 100% N_2, 10 °C/min of the heating rate, at 900 °C for 3 h, and performed the carbonation at 750 °C.

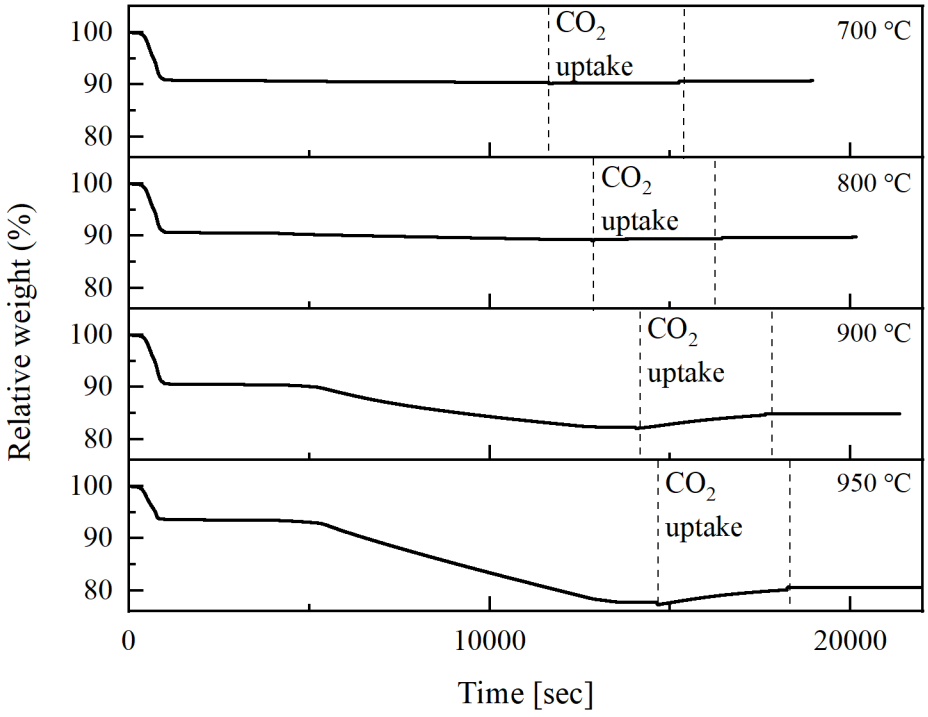

Figure S3. The synthesized K_2HfO_3 under 100% N_2, 10 °C/min of the heating rate, at 900 °C for 3 h, and performed the carbonation at 750 °C.

Table S1. The Calculated weight loss related to CO_2 elimination during the synthesis of NHO-Xs, assuming that the stoichiometry of the reaction mixture was as expected.

Na_2CO_3:HfO_2 ratio	Expected weight loss related to CO_2 elimination (%)
0.5:1	8.35
0.75:1	11.38
1:1	13.90
1.25:1	12.83
1.5:1	11.90

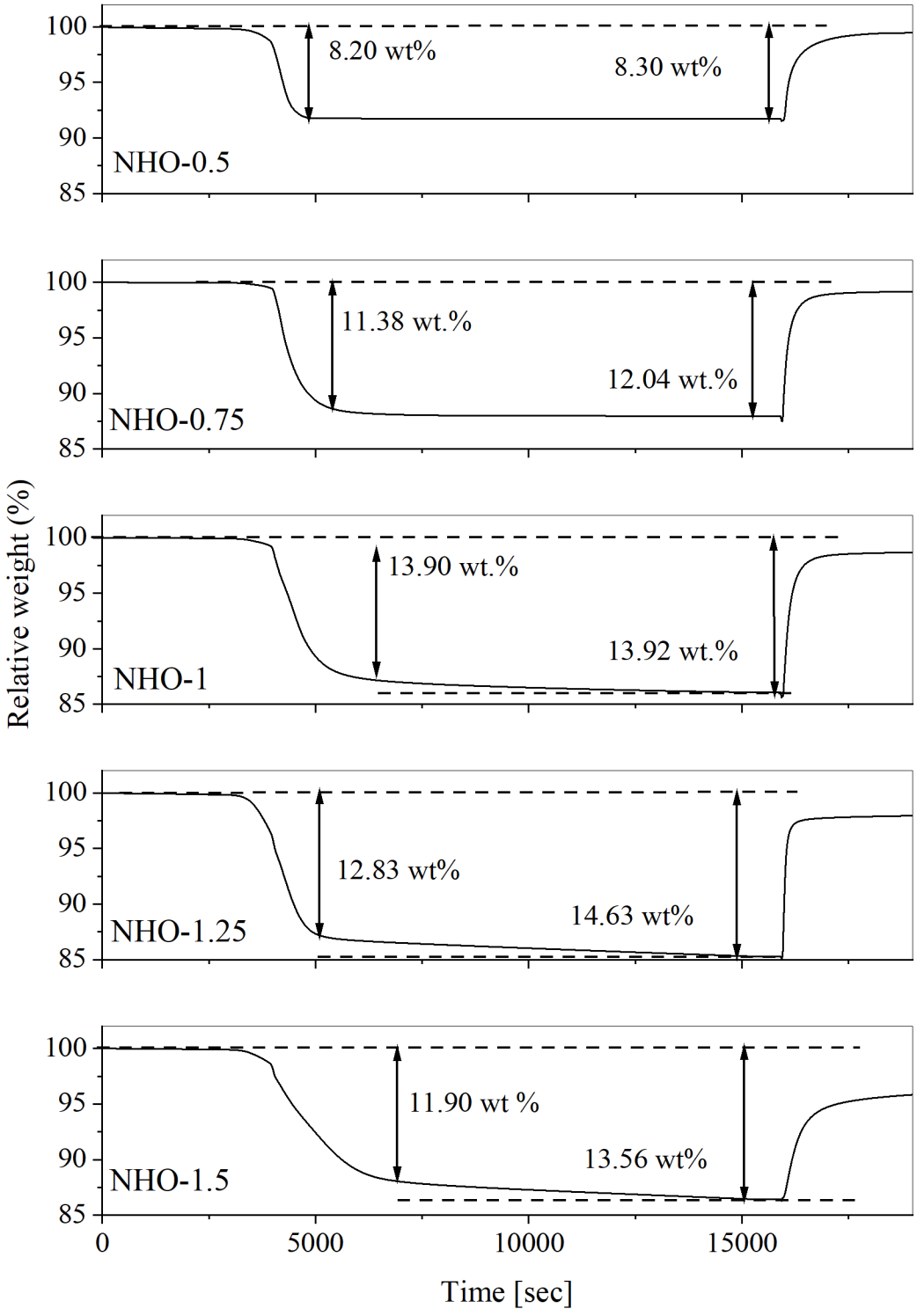

Figure S4. The Calculated weight loss related to CO_2 elimination during the synthesis of NHO-Xs, assuming that the stoichiometry of the reaction mixture was as expected (left arrow) and the recorded weight loss at the end of the 3h synthesis (right arrow). The differences are likely to be related to the over 100% theoretical maximum CO_2 uptake observed on some samples

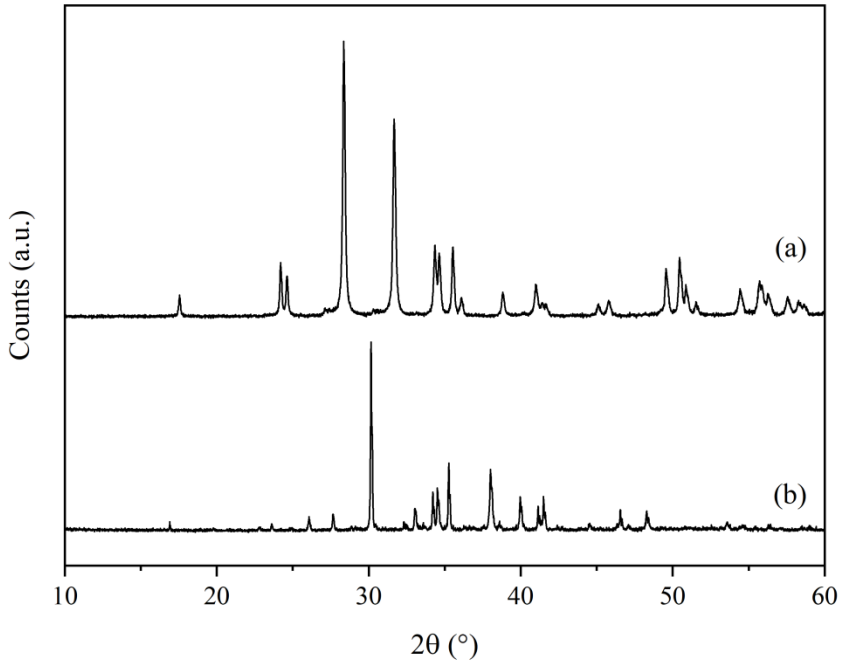

Figure S5. PXRD patterns of the starting materials of NHO-Xs (a) HfO_2 and (b) Na_2CO_3.

Table S2. Brunauer-Emmett-Teller (BET) specific surface area, Langmuir surface area, and average particle size of NHO-Xs.

NHOx	0.5	0.75	1	1.25	1.5
BET surface area[m^2/g]	3.83	3.76	3.51	3.66	2.83
Langmuir surface area [m^2/g]	5.56	6.32	5.53	8.88	5.59

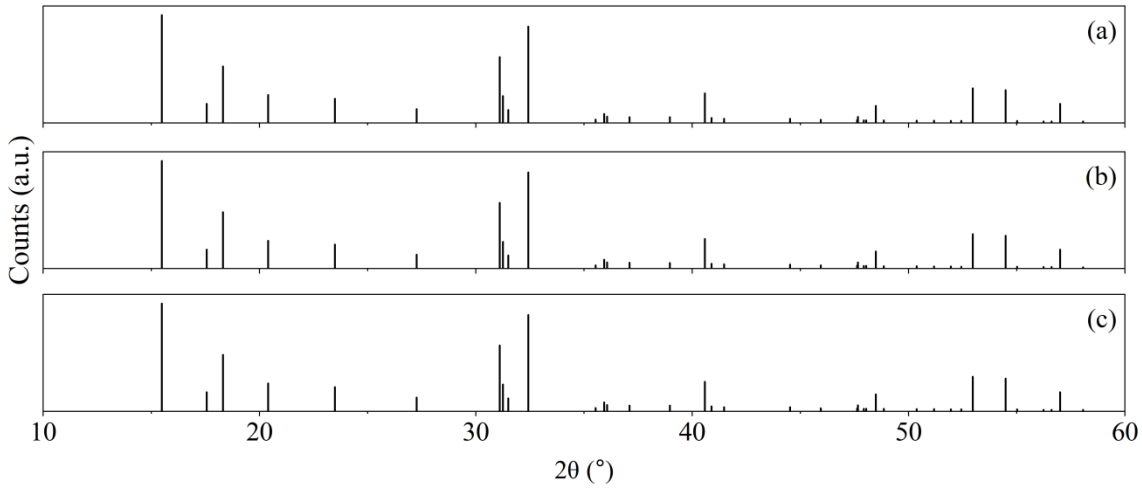

Figure S6. Simulated PXRD patterns of the three space groups (a) *C*2/m, (b) $P3_212$, and (c) $P3_112$, respectively.

Section 2. The effect of different carbonation temperatures

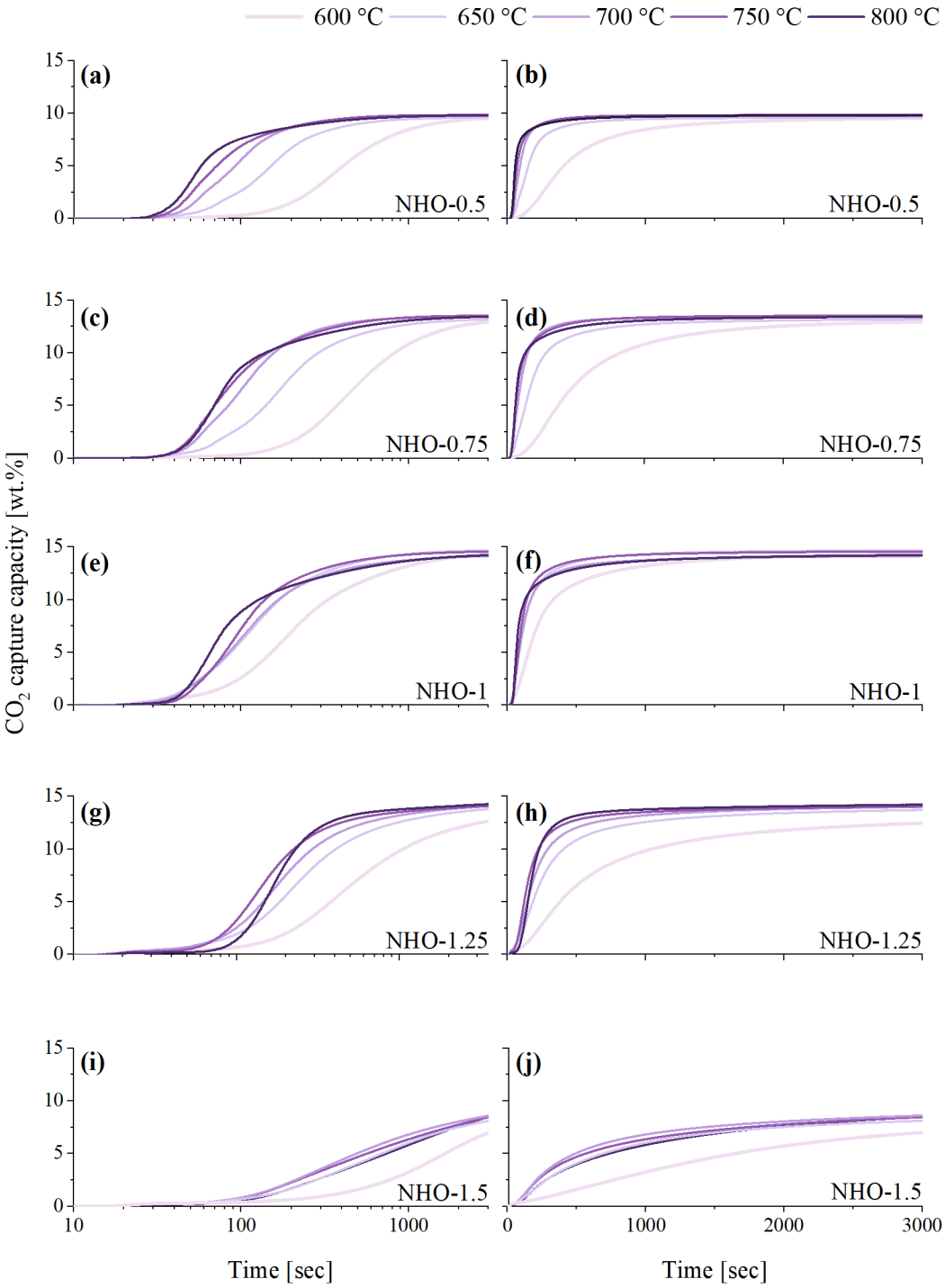

Figure S7. The CO_2 uptake capacity of different carbonation temperature (a and b) NHO-0.5 (c and d) NHO-0.75 (e and f) NHO-1 (f and h) NHO-1.25 (i and j) NHO-1.5.

Section 3. The effect of molar ratios between Na_2CO_3 and HfO_2

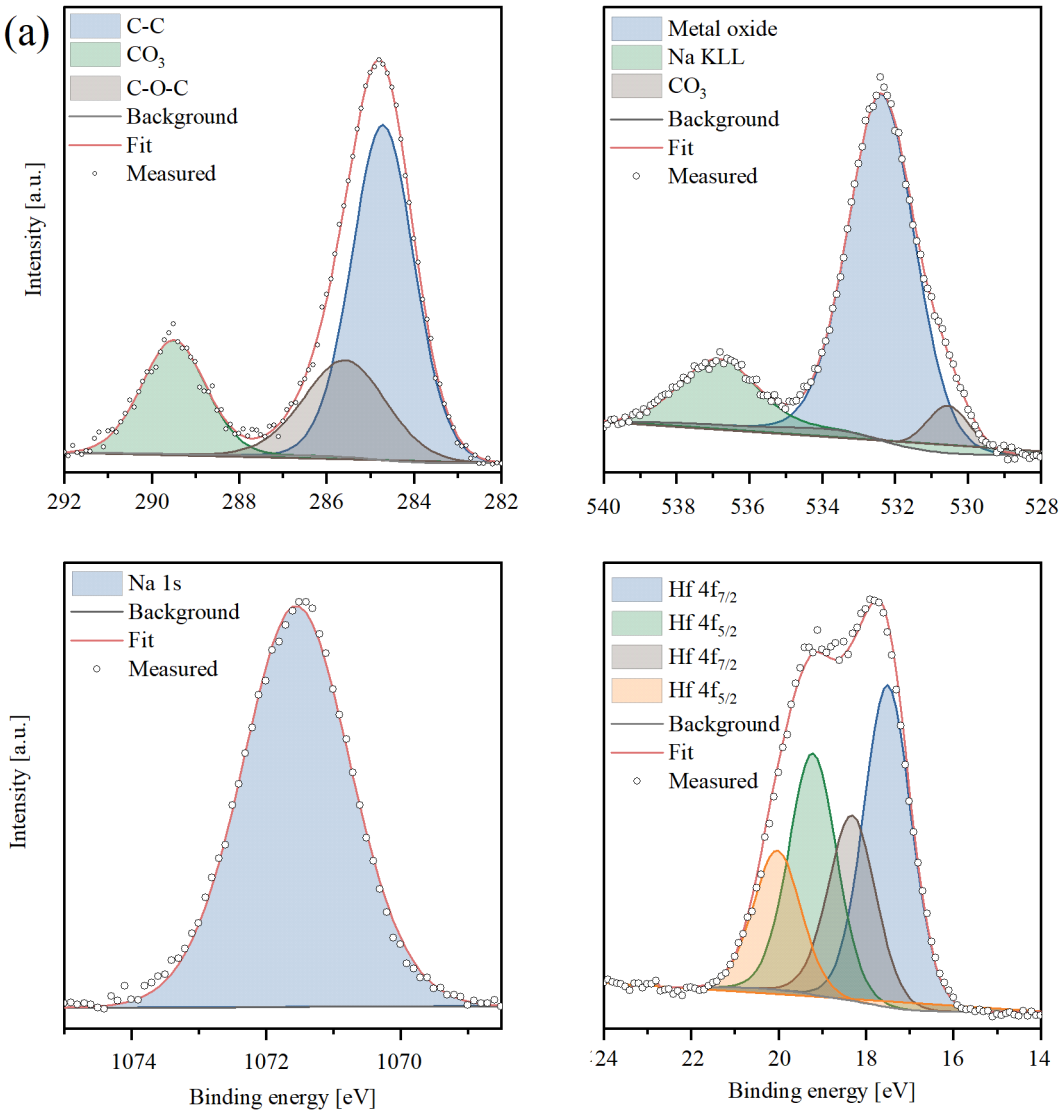

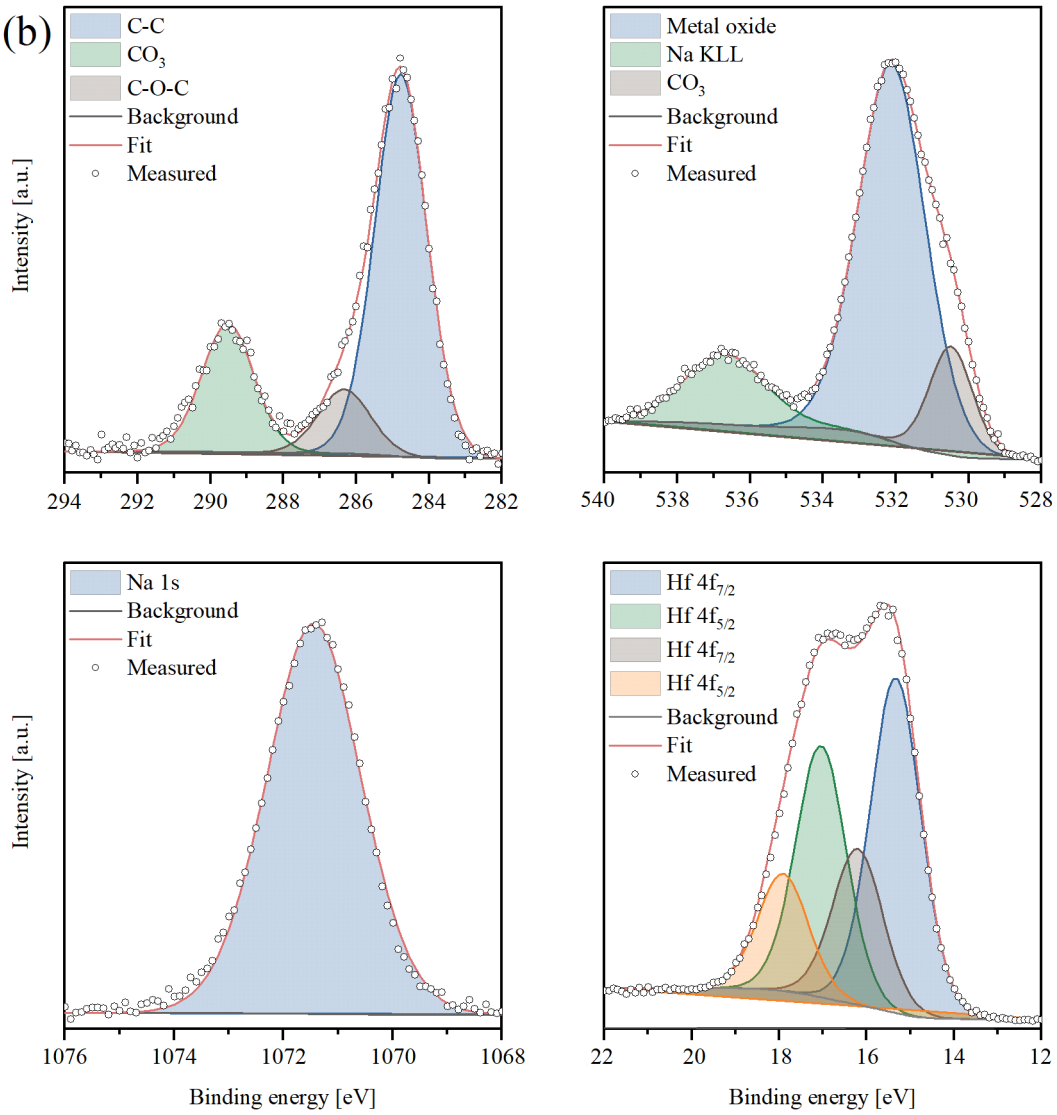
(b)
C-C
CO3
C-O-C
Background
Fit
Measured
Intensity [a.u.]
294
292
290
288
286
284
282
Metal oxide
Na KLL
CO3
Background
Fit
Measured
540
538
536
534
532
530
528
Na 1s
Background
Fit
Measured
Intensity [a.u.]
1076
1074
1072
1070
1068
Binding energy [eV]
Hf 4f7/2
Hf 4f5/2
Hf 4f7/2
Hf 4f5/2
Background
Fit
Measured
22
20
18
16
14
12
Binding energy [eV]

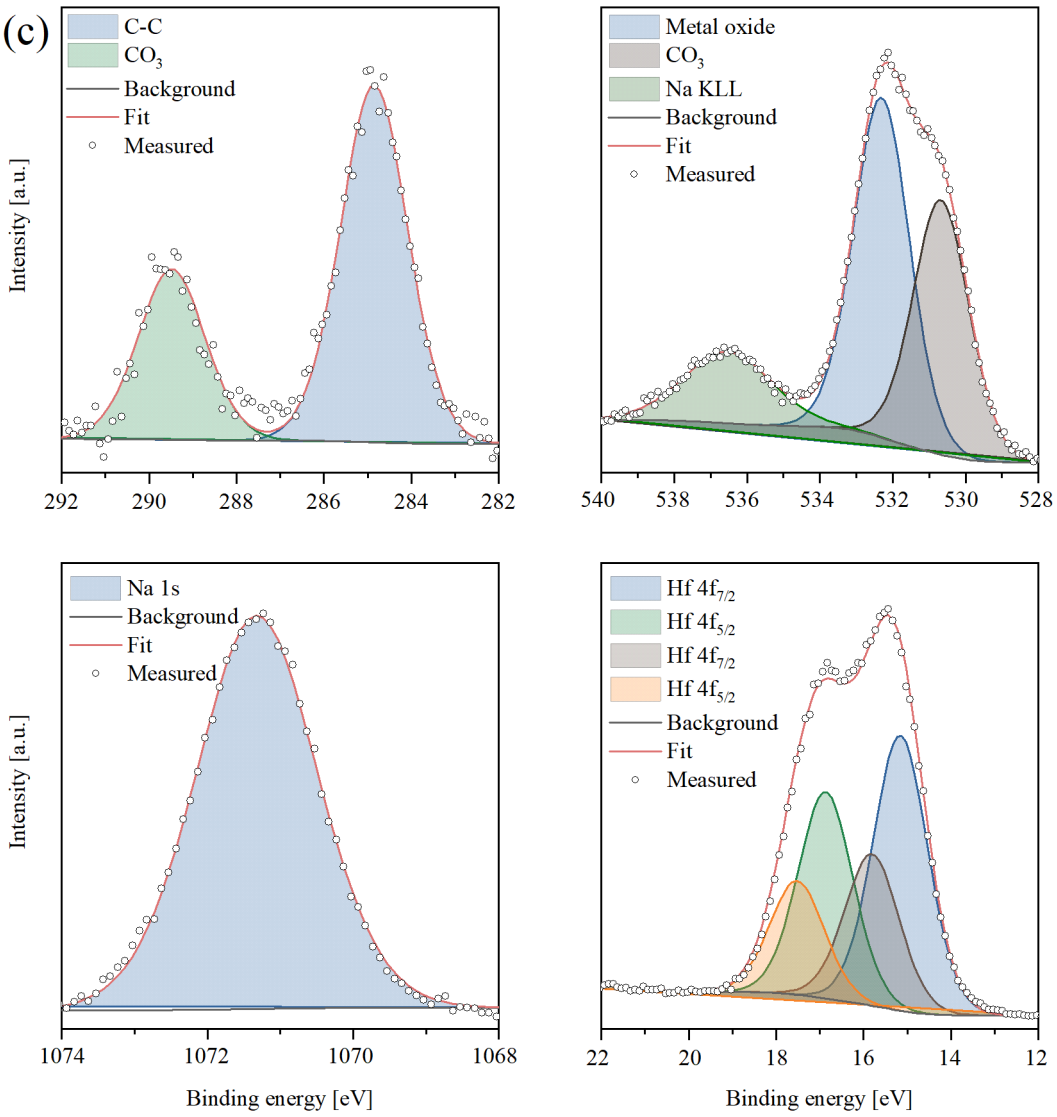
(c)
C-C
CO3
Background
Fit
Measured
Intensity [a.u.]
292
290
288
286
284
282
Metal oxide
CO3
Na KLL
Background
Fit
Measured
540
538
536
534
532
530
528
Na 1s
Background
Fit
Measured
Intensity [a.u.]
1074
1072
1070
1068
Binding energy [eV]
Hf 4f7/2
Hf 4f5/2
Hf 4f7/2
Hf 4f5/2
Background
Fit
Measured
22
20
18
16
14
12
Binding energy [eV]

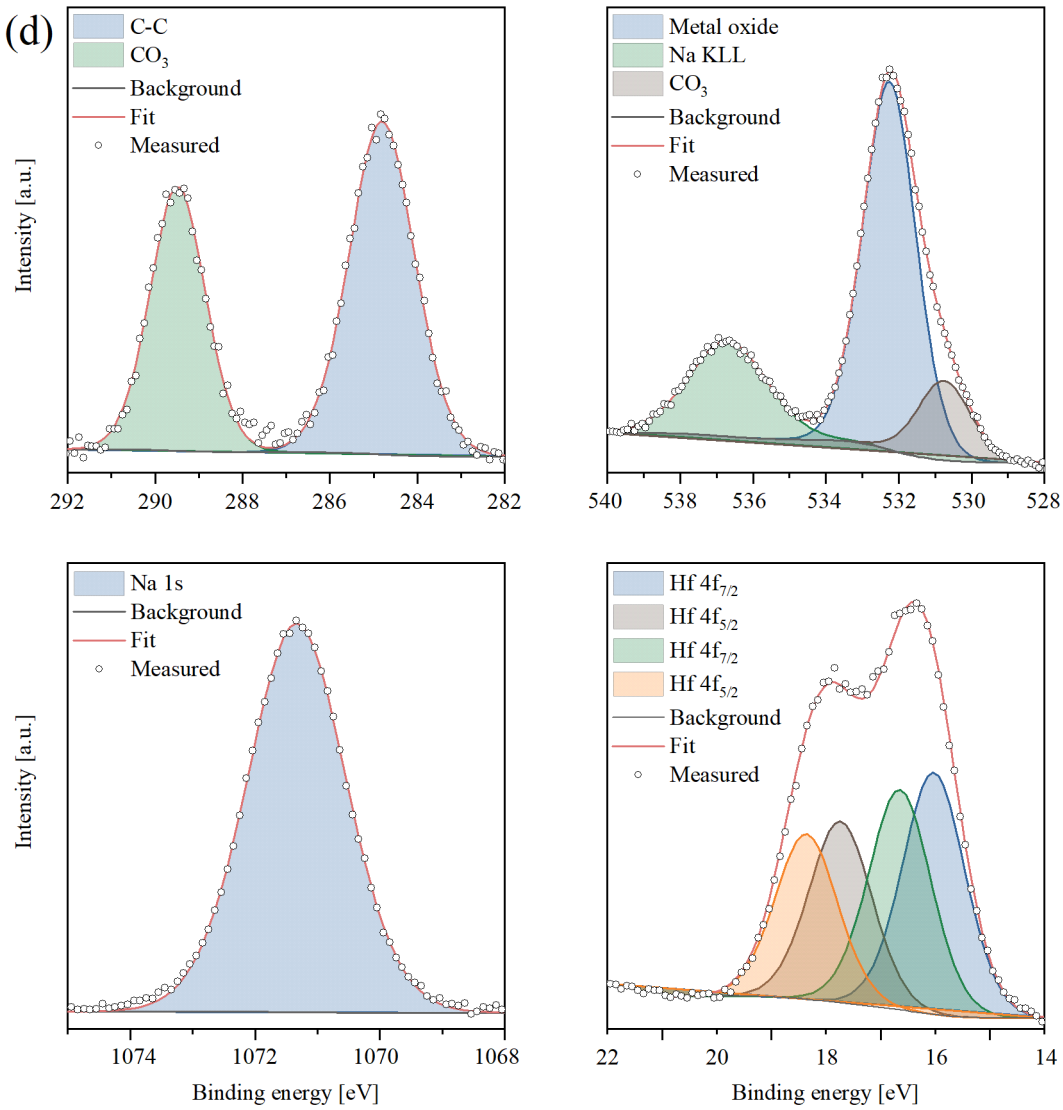
(d)
C-C
CO3
Background
Fit
Measured
Intensity [a.u.]
292
290
288
286
284
282
Metal oxide
Na KLL
CO3
Background
Fit
Measured
540
538
536
534
532
530
528
Na 1s
Background
Fit
Measured
Intensity [a.u.]
1074
1072
1070
1068
Binding energy [eV]
Hf 4f7/2
Hf 4f5/2
Hf 4f7/2
Hf 4f5/2
Background
Fit
Measured
22
20
18
16
14
Binding energy [eV]

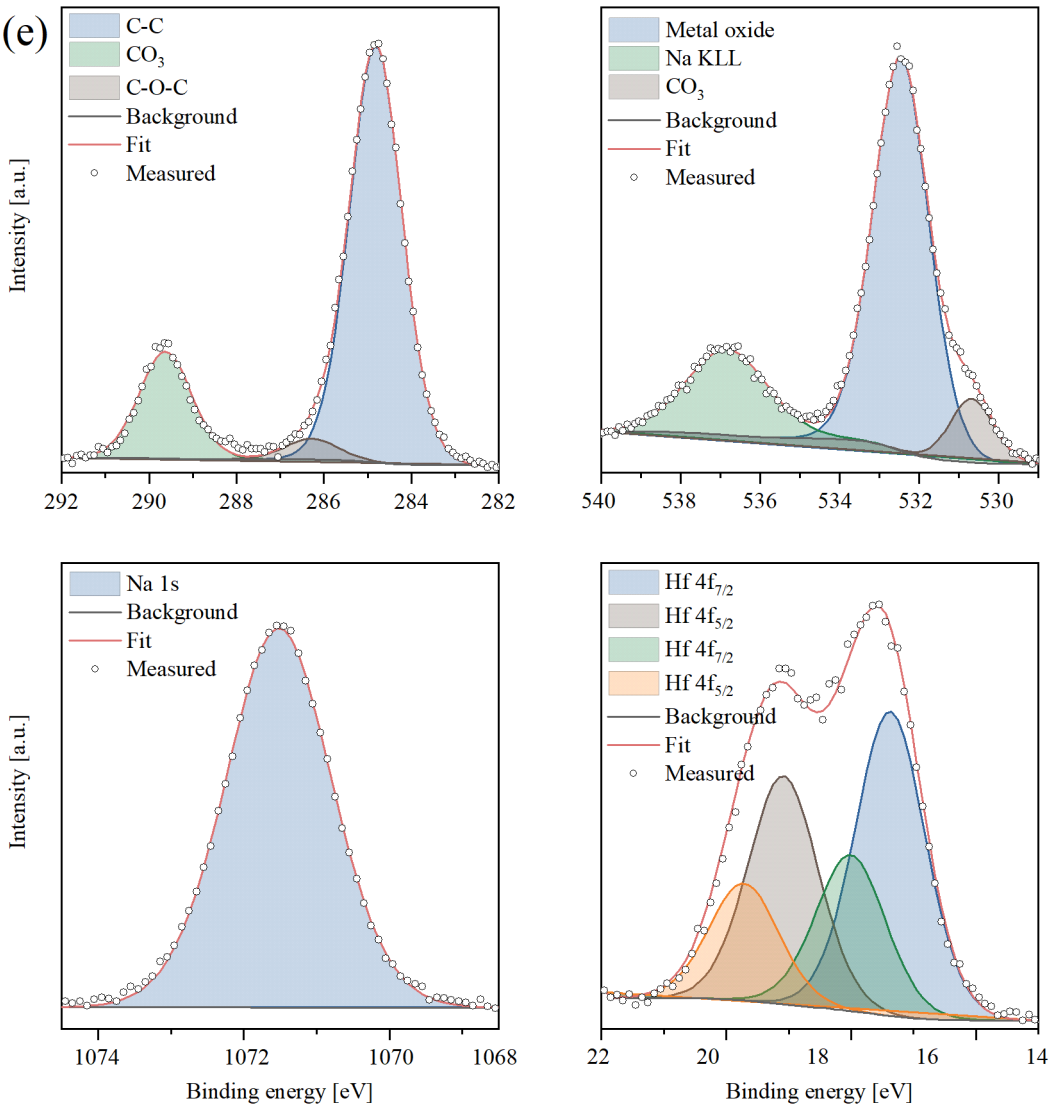

Figure S8. XPS spectra of the synthesized NHO-Xs (a) NHO-0.5 (b) NHO-0.75 (c) NHO-1 (d) NHO-1.25 (e) NOH-1.5.

Section 4. The effect of synthesis time/heating rate

Table S3. The CO_2 uptake capacity of the synthesized NHO-Xs by different synthesis times and heating rates.

Sorbent	Synthesis time [hr]	Theoretical max CO_2 uptake [wt.%]	Recorded CO_2uptake [wt.%]	Recorded uptake vs theoretical uptake [%]	Reference
NHO-0.5	1	9.1	11.91	130.88	This work
NHO-0.5	2	9.1	7.79	85.60	This work
NHO-0.5	3	9.1	7.02	77.14	This work
NHO-0.5	4	9.1	6.53	71.76	This work
NHO-0.75	1	12.8	9.21	71.95	This work
NHO-0.75	2	12.8	11.02	86.09	This work
NHO-0.75	3	12.8	12.45	97.27	This work
NHO-0.75	4	12.8	11.56	90.31	This work
NHO-1	1	16.1	13.97	86.77	This work
NHO-1	2	16.1	15.1	93.79	This work
NHO-1	3	16.1	14.87	92.36	This work
NHO-1	4	16.1	14.64	90.93	This work
NHO-1.25	1	14.7	13.33	90.68	This work
NHO-1.25	2	14.7	13.09	89.05	This work
NHO-1.25	3	14.7	15.18	103.27	This work
NHO-1.25	4	14.7	11.05	75.17	This work
NHO-1.5	1	13.5	6	44.44	This work
NHO-1.5	2	13.5	9.95	73.70	This work
NHO-1.5	3	13.5	8.04	59.56	This work
NHO-1.5	4	13.5	9.45	70.00	This work
Sorbent	Heating rate [°C/min]	Theoretical max CO_2 uptake [wt.%]	Recorded CO_2uptake [wt.%]	Recorded uptake vs theoretical uptake [%]	Reference
NHO-1	2	16.1	15.03	93.35	This work
NHO-1	5	16.1	15.09	93.73	This work
NHO-1	10	16.1	15.1	93.79	This work
NHO-1.25	2	14.7	13.09	89.05	This work
NHO-1.25	5	14.7	15.17	103.20	This work
NHO-1.25	10	14.7	15.17	103.20	This work

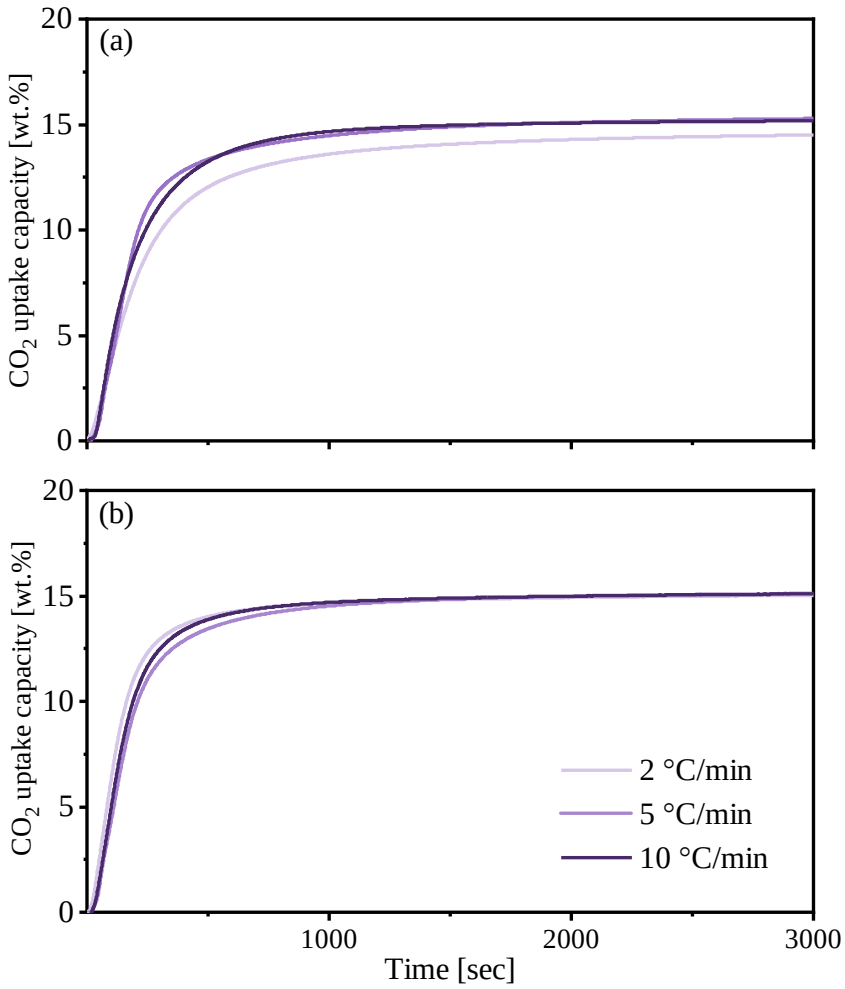

Figure S9. The CO_2 uptake capacity of the synthesized (a) NHO-1.25 and (b) NHO-1 with different heating rates of 2, 5, 10 °C/min.

Section 5. cyclic stability

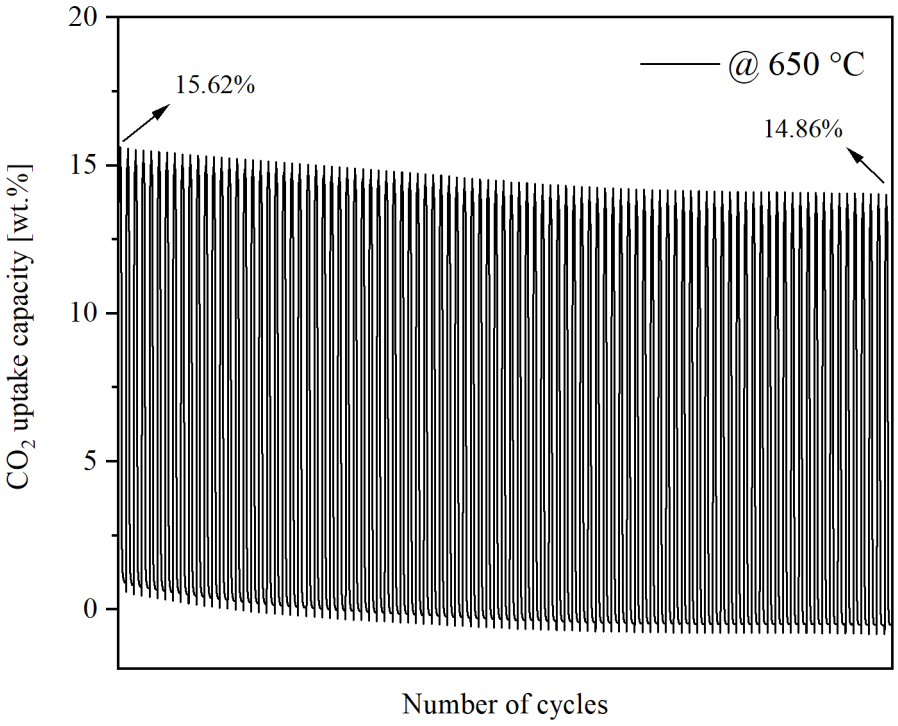

Figure S10. The cycle stability of NHO-1 under optimized conditions: synthesis at 900 °C for 2hrs; carbonation and calcination at 650 and 900 °C for 20 and 20 min with 10 °C/min of heating.

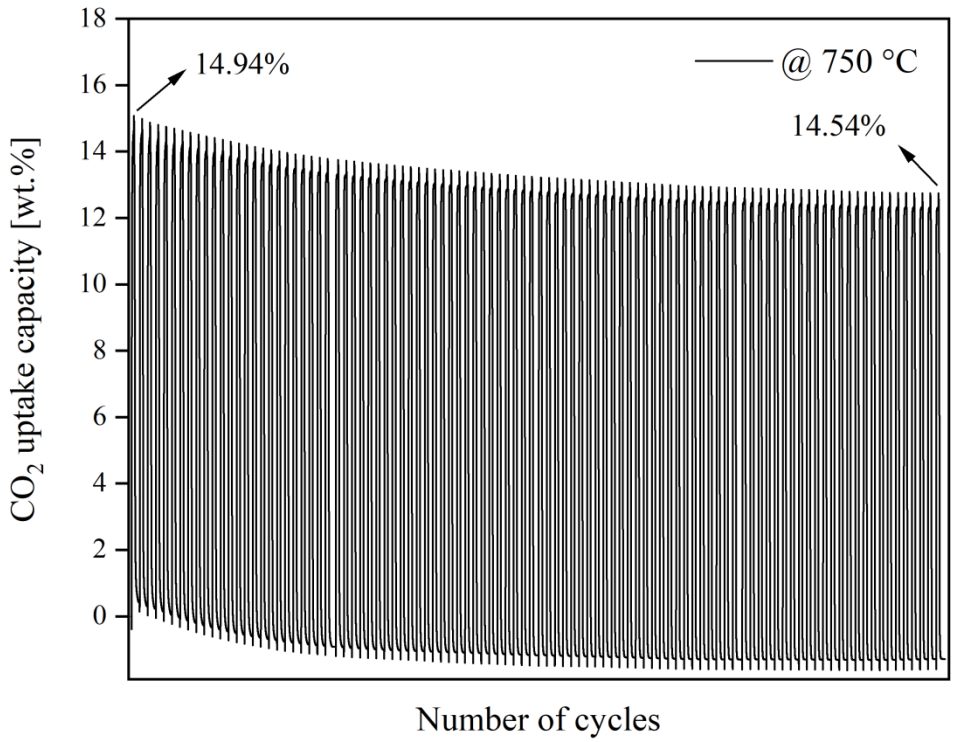

Figure S11. The cycle stability of NHO-1.25 under optimized conditions: synthesis at 900 °C for 3hrs; carbonation and calcination at 750 and 900 °C for 20 and 20 min with 10 °C/min of heating.

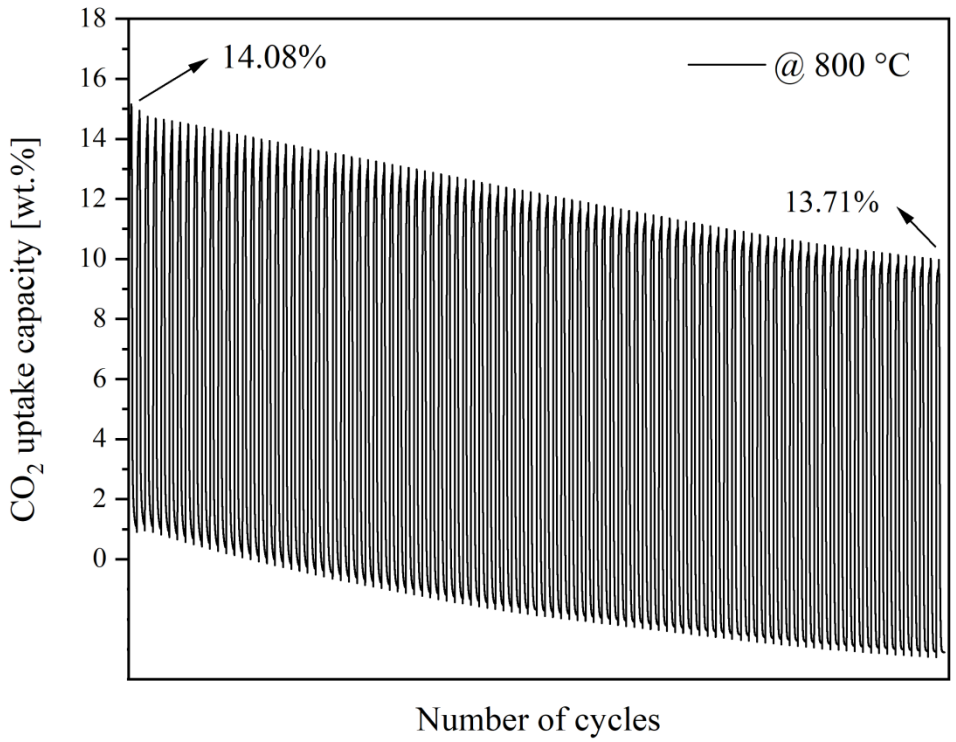

Figure S12. The cycle stability of NHO-1.25 under optimized conditions: synthesis at 900 °C for 3hrs; carbonation and calcination at 800 and 900 °C for 20 and 20 min with 10 °C/min of heating.

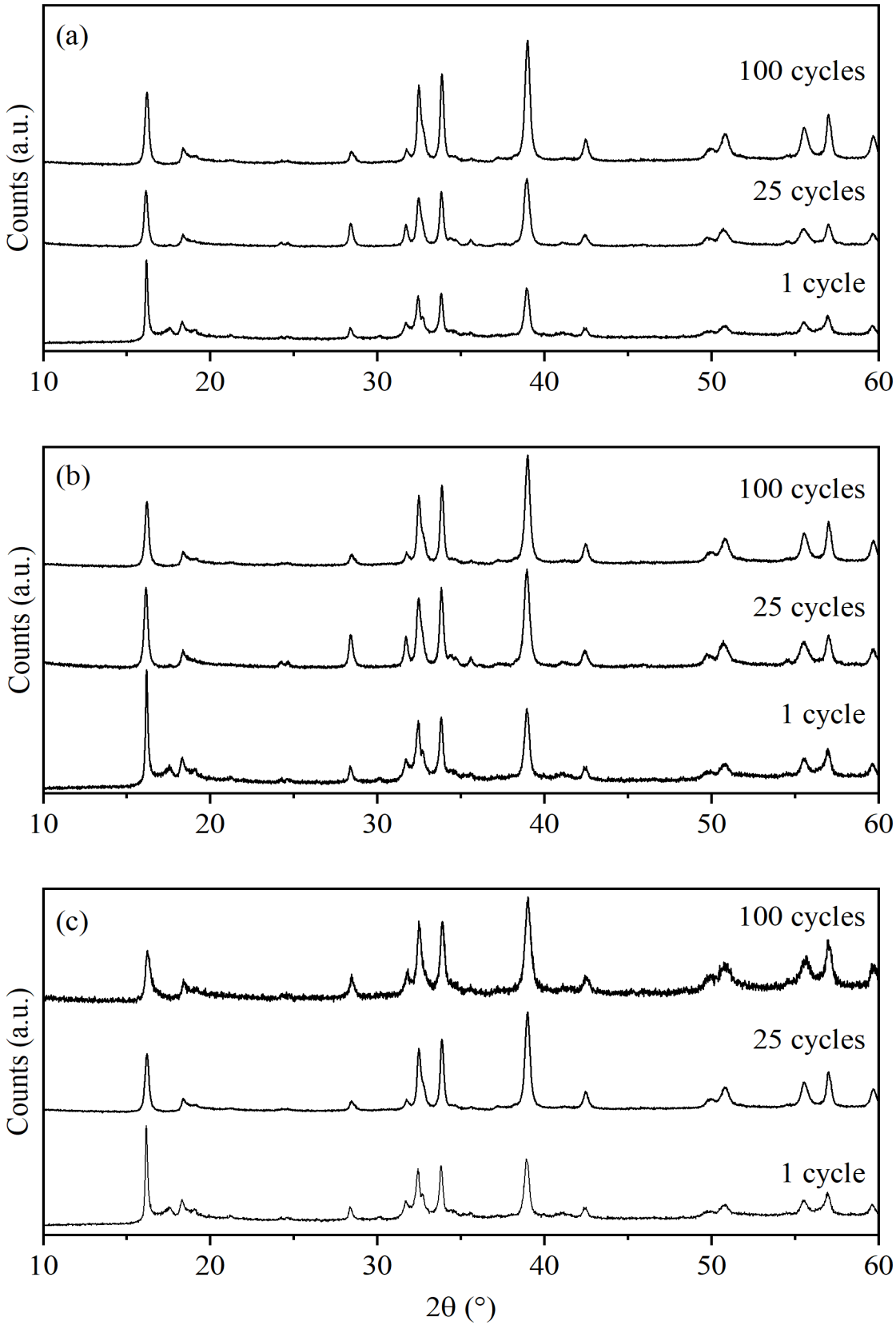

Figure S13. PXRD patterns after the cyclic stability test of (a) NHO1.25 at 750, (b) NHO1.25 at 800, and (c) NHO1 at 650 °C.

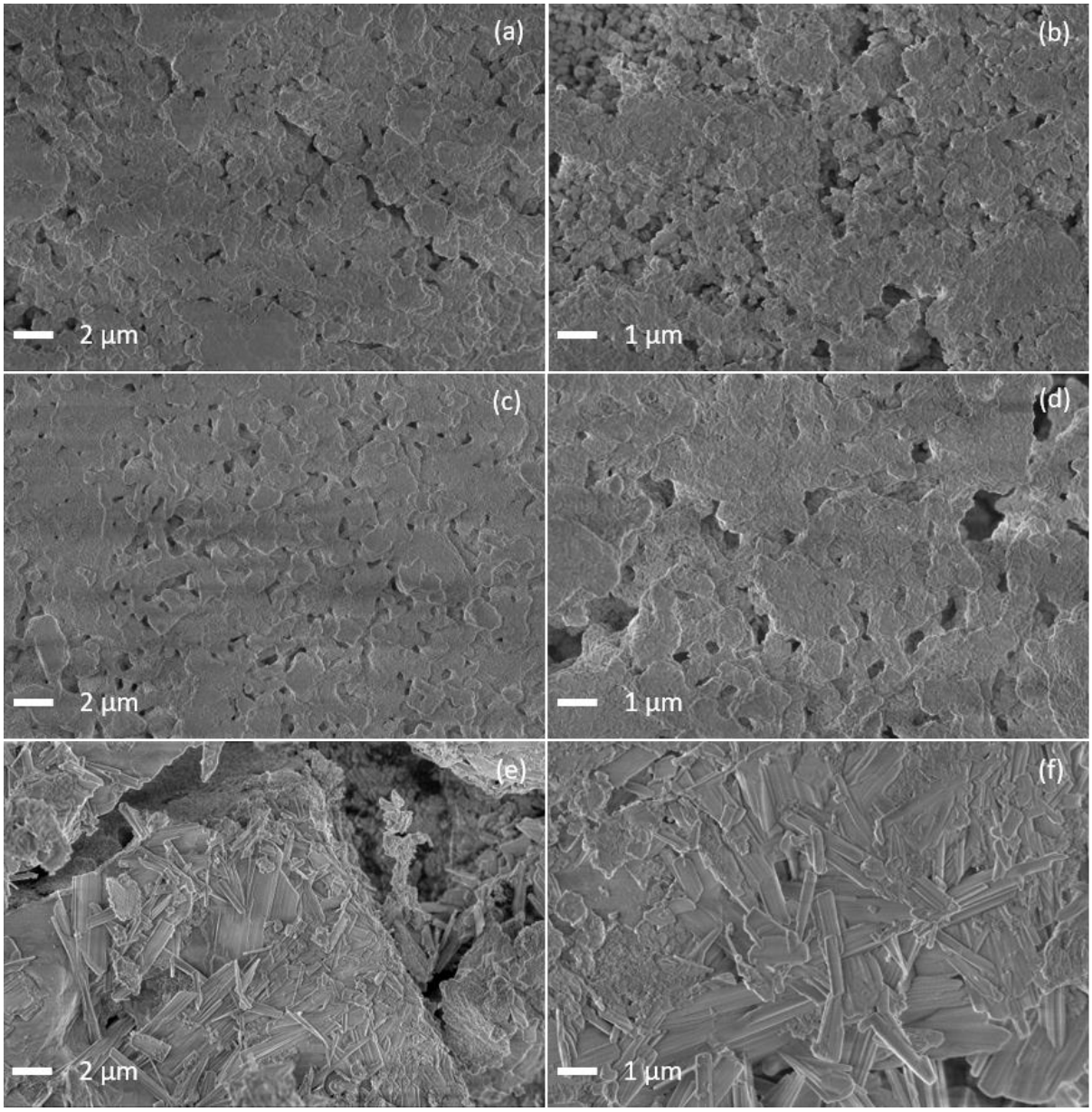

Figure S14. SEM images of the sorbent synthesized with 1.25:1 ratio under optimized conditions: synthesis at 900 °C for 3hrs; carbonation and calcination at 800 and 900 °C for 20 and 20 min with 10 °C/min of heating (a and b) 5 cycles (c and d) 100 cycles (e and f) After carbonation.

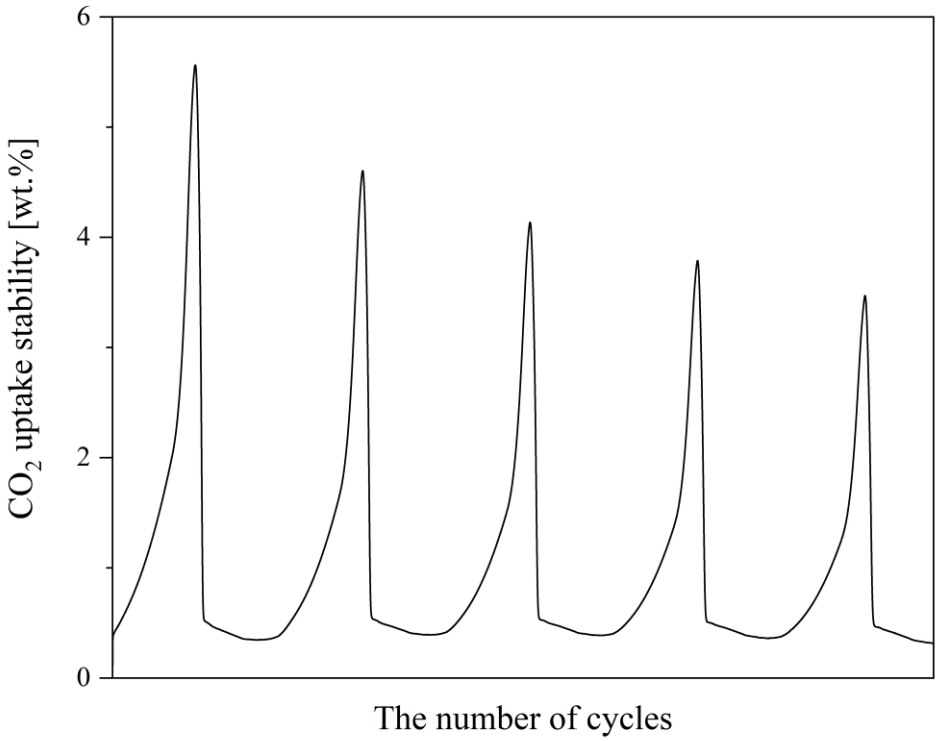

Figure S15. The CO_2 uptake capacity and stability of NHO-1.25 under the mixed gas conditions for carbonation and calcination at 600 and 1000 °C for 30 and 60 min.

Section 6. Kinetic analysis on NHO-Xs

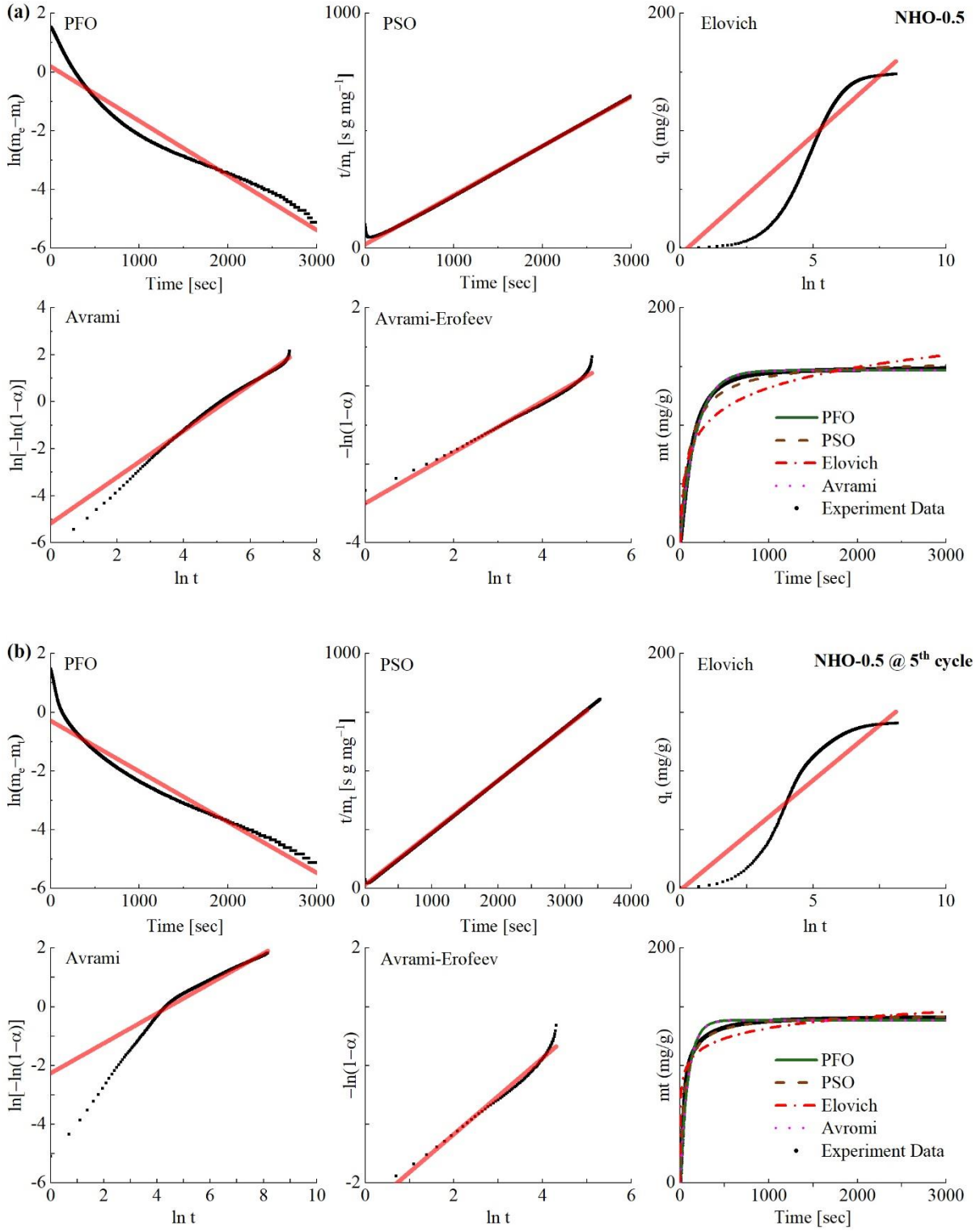

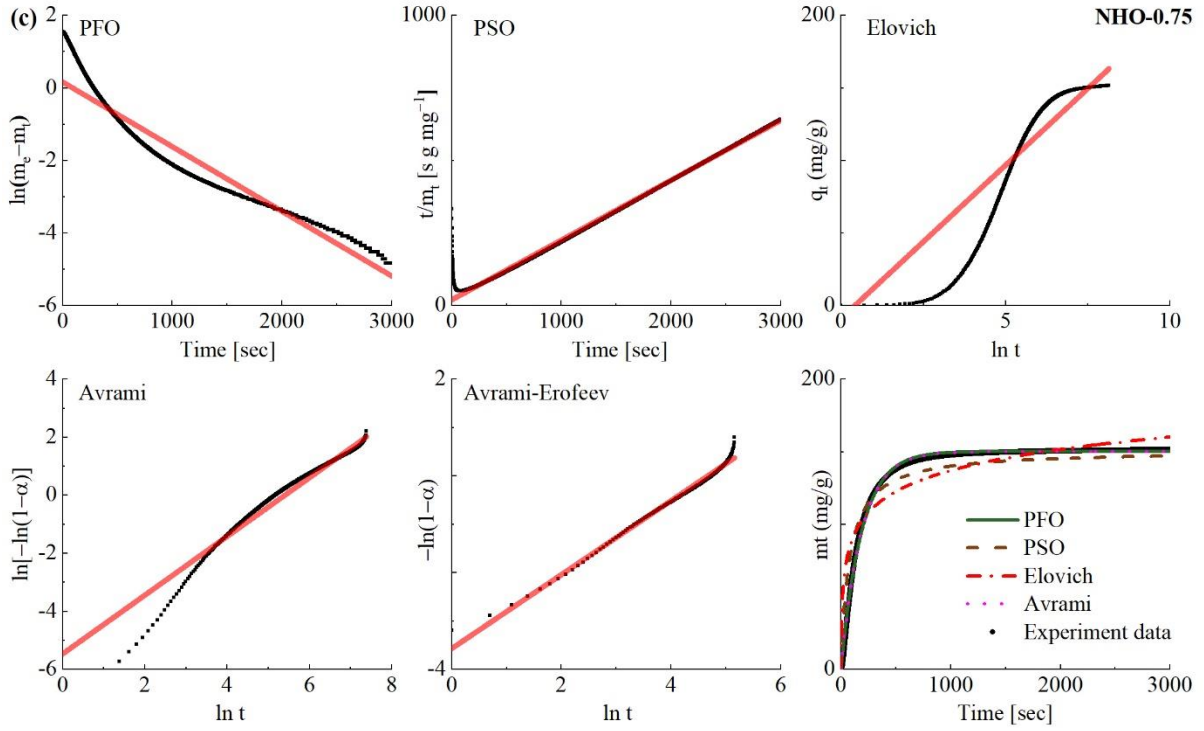
(c)
PFO
PSO
Elovich
NHO-0.75
Avrami
Avrami-Erofeev
Time [sec]
ln t
mt (mg/g)
PFO
PSO
Elovich
Avrami
Experiment data

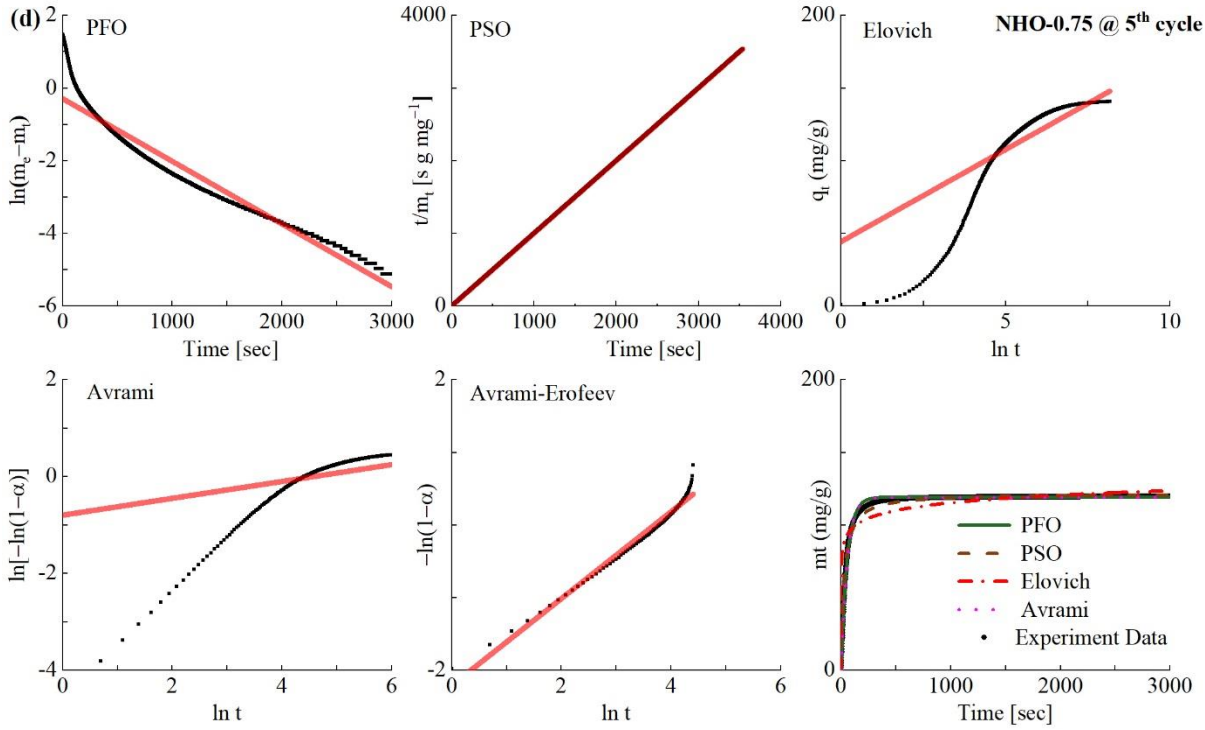
(d)
PFO
PSO
Elovich
NHO-0.75 @ 5th cycle
Avrami
Avrami-Erofeev
Time [sec]
ln t
mt (mg/g)
PFO
PSO
Elovich
Avrami
Experiment Data

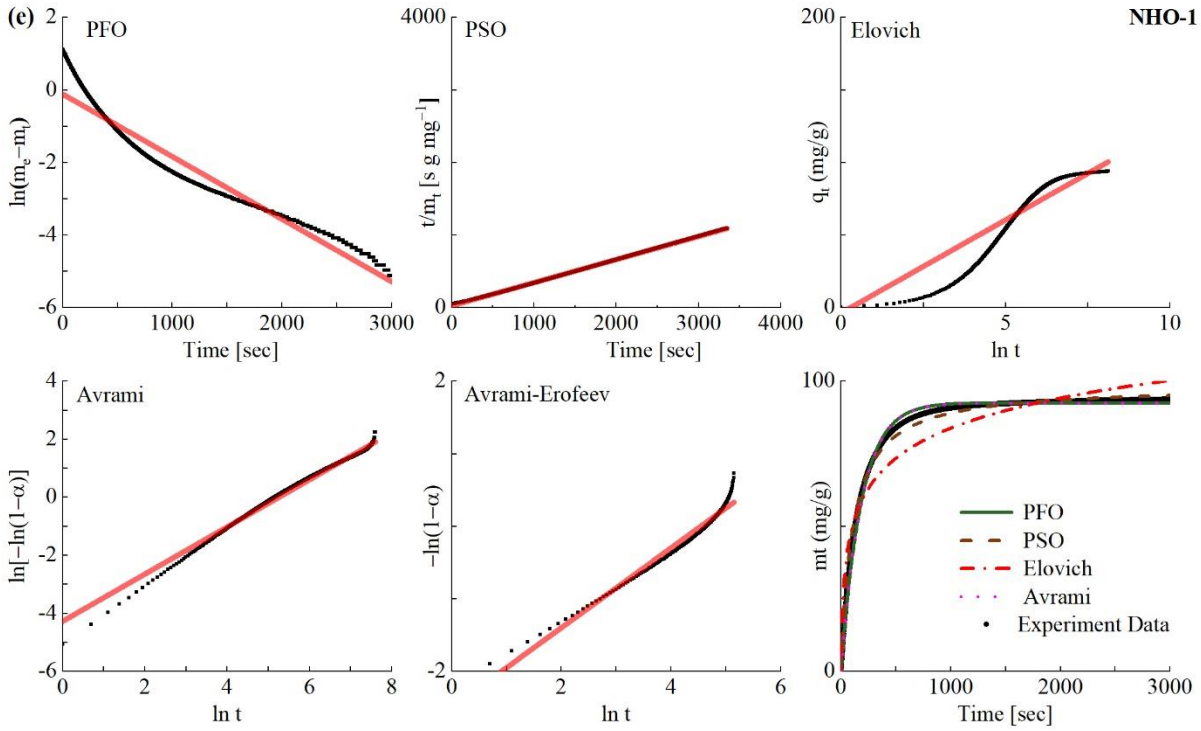
(e)
NHO-1
PFO
PSO
Elovich
Avrami
Avrami-Erofeev
ln(m_e−m_t)
t/m_t [s g mg^−1]
q_t (mg/g)
ln[−ln(1−α)]
−ln(1−α)
mt (mg/g)
Time [sec]
ln t
PFO
PSO
Elovich
Avrami
Experiment Data

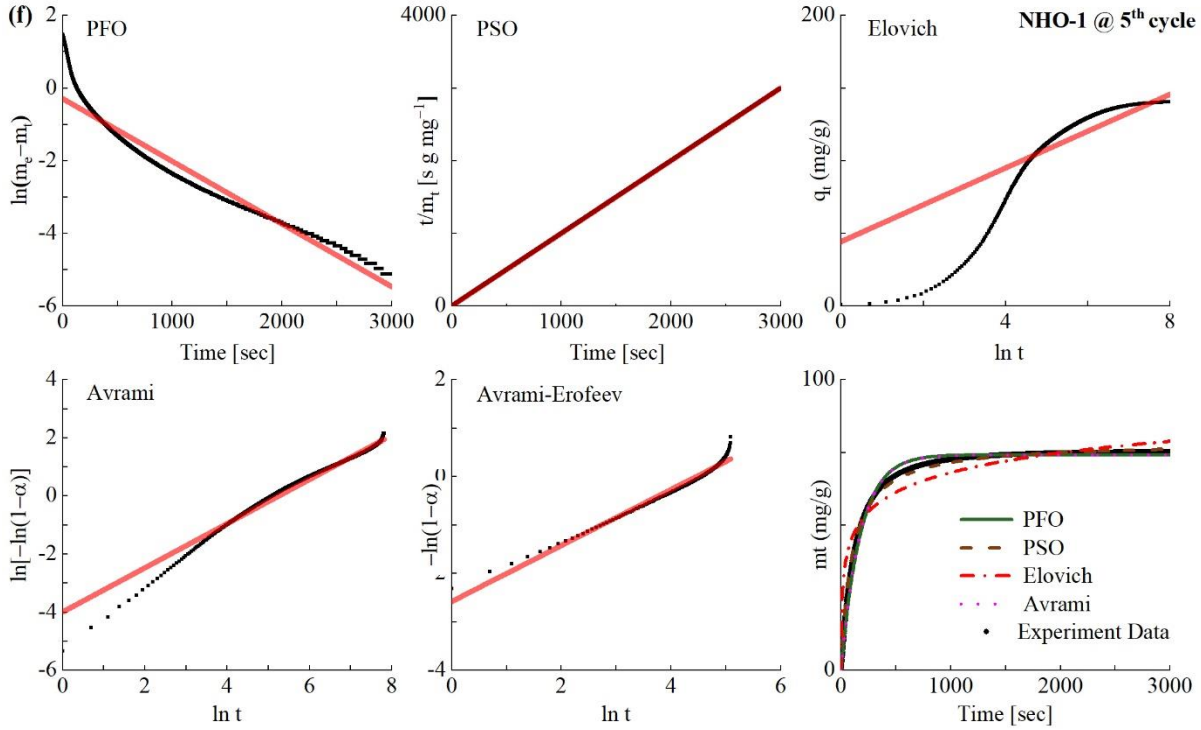
(f)
NHO-1 @ 5th cycle
PFO
PSO
Elovich
Avrami
Avrami-Erofeev
ln(m_e−m_t)
t/m_t [s g mg^−1]
q_t (mg/g)
ln[−ln(1−α)]
−ln(1−α)
mt (mg/g)
Time [sec]
ln t
PFO
PSO
Elovich
Avrami
Experiment Data

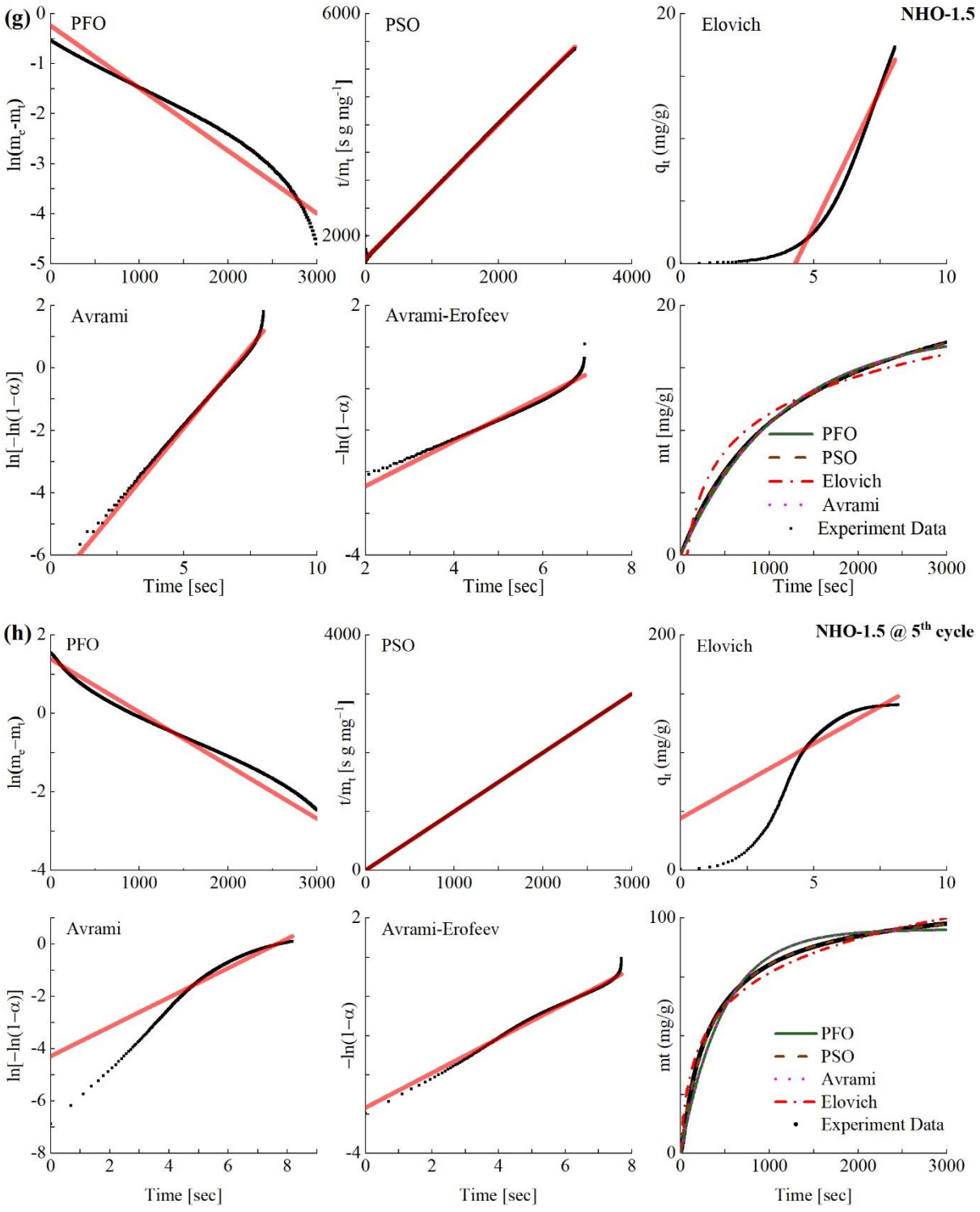

Figure S16. The CO_2 uptake kinetics of the synthesized NHO-Xs using five different kinetic models; the pseudo first order (PFO) model, pseudo second order (PSO) model, the Elovich model, the Avrami model and the Avrami-Erofeev for (a) NHO-0.5, (b) NHO-0.75, (c) NHO-1, (d) NHO-1.25, (e) NHO-1.5.

Table S4. The correlation coefficient (R^2) and Root-MSE of five different kinetic models; the pseudo first order (PFO) model, pseudo second order (PSO) model, the Elovich model, the Avrami model and the Avrami-Erofeev for the synthesized NHO-Xs from 1st and 5th cycles.

Sorbents	R^2 from linear type				
	PFO	PSO	Avrami	Avrami_E	Elovich
NHO-0.5	0.97343	0.99955	0.9935	0.9895	0.89058
NHO-0.75	0.97221	0.99747	0.98286	0.99432	0.88592
NHO-1	0.97576	0.99986	0.98368	0.99435	0.91073
NHO-1.25	0.96736	0.99982	0.95689	0.98219	0.87867
NHO-1.5	0.94535	0.99972	0.99062	0.97814	0.96
NHO-0.5 at 5th cycles	0.9807	0.9998	0.96446	0.98702	0.8943
NHO-0.75 at 5th cycles	0.98	1	0.68203	0.98757	0.84969
NHO-1 at 5th cycles	0.9807	1	0.98182	0.9901	0.84969
NHO-1.25 at 5th cycles	0.9807	1	0.96446	0.98681	0.84969
Sorbents	Root-MSE from Non-linear type				
	PFO	PSO	Avrami	Elovich	
NHO-0.5	1.54628	3.88721	1.54628	13.16562	
NHO-0.75	1.63853	8.52559	1.63853	11.10093	
NHO-1	1.42262	1.75178	1.42262	4.95774	
NHO-1.25	2.4	2.86196	2.4	8.43823	
NHO-1.5	0.22512	0.03543	0.22512	1.24756	
NHO-0.5 at 5th cycles	3.19	1.58487	3.19	7.82237	
NHO-0.75 at 5th cycles	1.20689	1.98355	1.20689	6.95818	
NHO-1 at 5th cycles	3.14634	1.88803	3.14634	8.21768	
NHO-1.25 at 5th cycles	1.41966	1.13866	1.41966	4.50027	
NHO-1.5 at 5th cycles	3.05931	0.43835	3.05931	2.9943	

Section 7. 3D printing

Table S5. The conditions of the 3D-printer for the printed structure of NHO-1

Printing parameter	Value
Layer height, mm	0.15
Wall line count	1
Infill type	Zig Zag
Infill density, %	20
Printing speed, mm/s	3 mm/s
Printing surface temperature, ˚C	60

The 3D model was created in Fusion 360 (Autodesk, San Francisco, USA) and transferred to Ultimaker Cura 5.1.0 (Ultimaker B.V, Utrecht, Netherlands) for the following printing protocol generation. Then, the printing parameters (Table S5) were set and the final G-code file was created. After that, the loaded syringe with a tip was loaded into the tool head and the model was built on the glass cover sleep covered with an alumina foil for better material adhesion. The pre-heated printing surface prevent the extruded material from uncontrolled spreading what consequently increase the overall resolution.

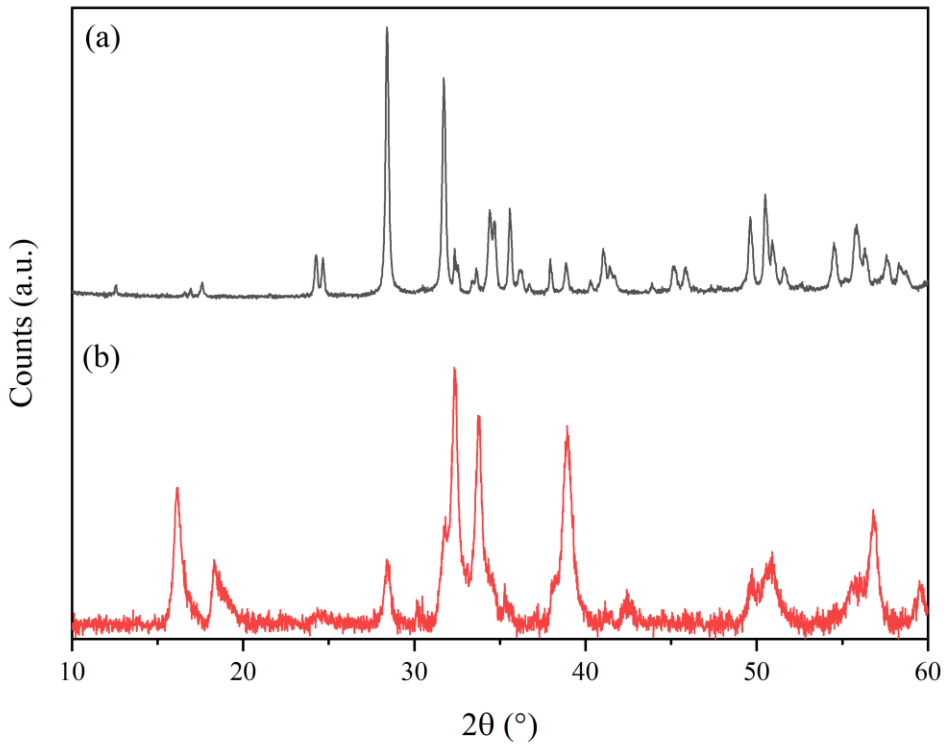

Figure S17. PXRD patterns of the 3D-printed NHO-1 (a) before synthesis (b) after synthesis.

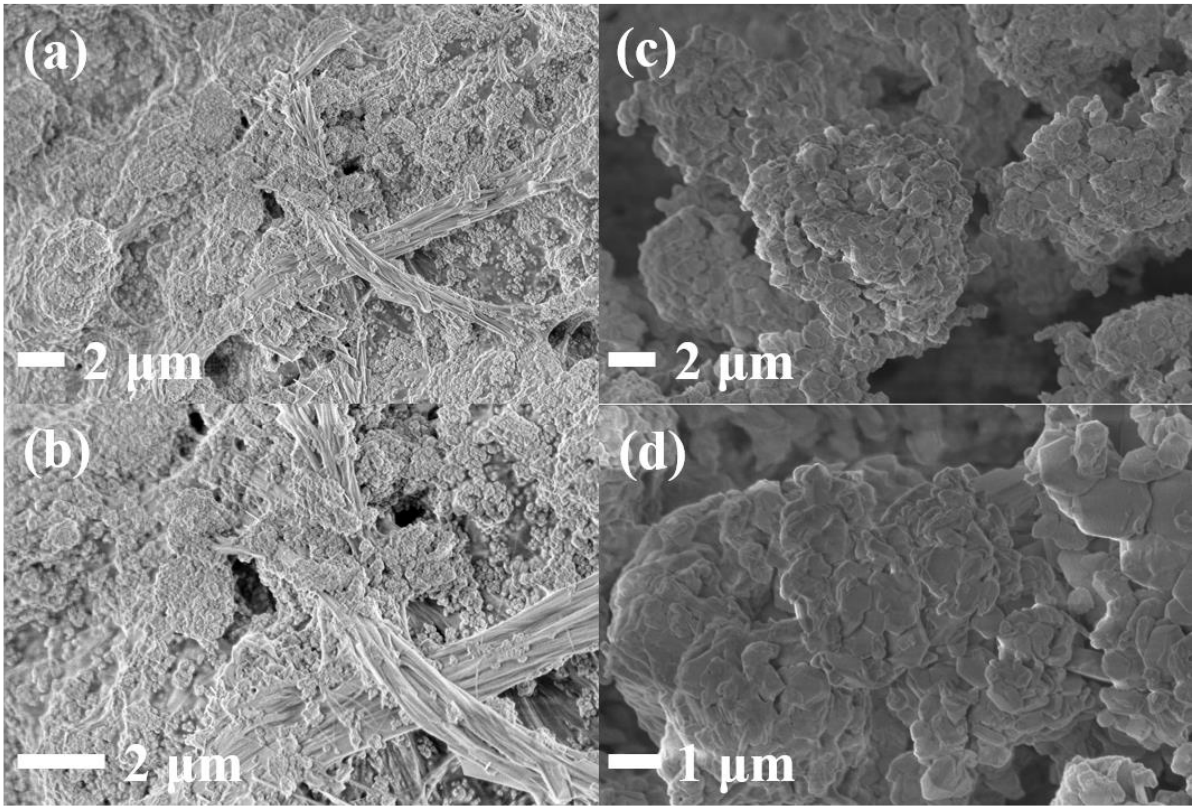

Figure S18. SEM images of the 3D-printed NHO-1 (a and b) before synthesis (c and d) after synthesis.

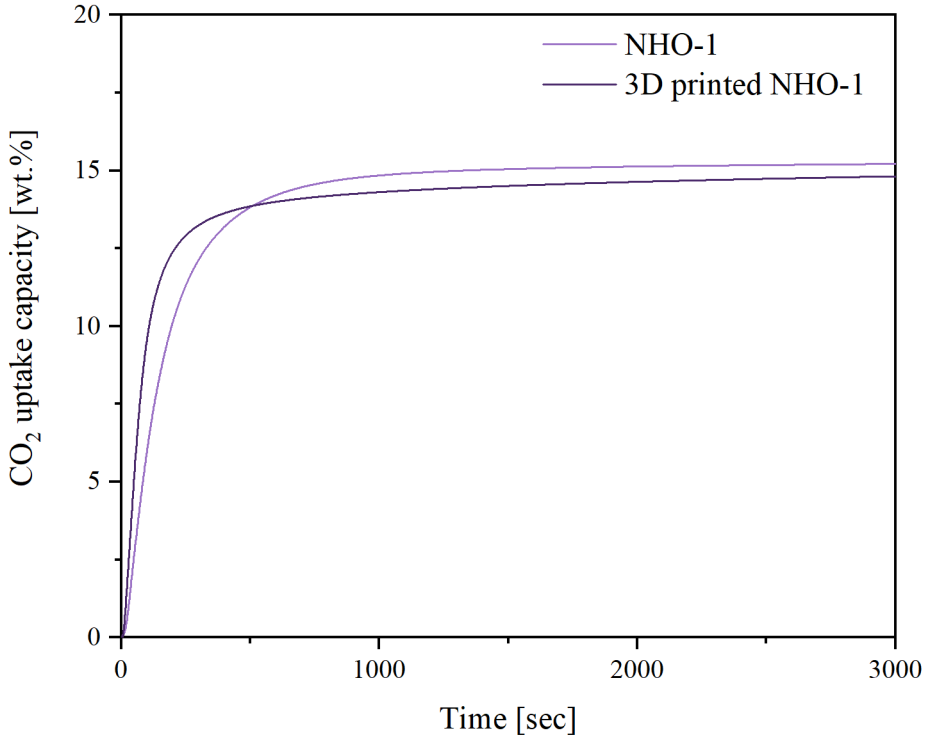

Figure S19. The CO_2 uptake capacity of the 3D-printed NHO-1.

Table S6. Brunauer-Emmett-Teller (BET) specific surface area, Langmuir surface area, and average particle size of the 3D printed NHO-1.

NHOx	NHO-1	3D printed NHI-1
BET surface area[m^2/g]	3.50	5.06
Langmuir surface area [m^2/g]	5.53	8.64